

LARGE-AMPLITUDE, PAIR-CREATING OSCILLATIONS IN PULSAR AND BLACK HOLE MAGNETOSPHERES

AMIR LEVINSON,¹ DON MELROSE,² ALEX JUDGE,² AND QINGHUAN LUO²

Received 2005 March 14; accepted 2005 May 27

ABSTRACT

A time-dependent model for pair creation in a pulsar magnetosphere is developed in which the parallel electric field oscillates with large amplitude. Electrons and positrons are accelerated periodically, and the amplitude of the oscillations is assumed to be large enough to cause creation of upgoing and downgoing pairs at different phases of the oscillation. With a charge-starved initial condition, we find that the oscillations result in bursts of pair creation in which the pair density rises exponentially with time. The pair density saturates at $N_{\pm} \simeq E_0^2 / (8\pi m_e c^2 \Gamma_{\text{thr}})$, where E_0 is the parallel electric field in the charge-starved initial state and Γ_{thr} is the Lorentz factor for effective pair creation. The frequency of oscillations following the pair creation burst is given roughly by $\omega_{\text{osc}} = eE_0 / (8m_e c \Gamma_{\text{thr}})$. A positive feedback keeps the system stable, such that the average pair creation rate balances the loss rate due to pairs escaping the magnetosphere.

Subject headings: black hole physics — magnetic fields — plasmas — pulsars: general — radio continuum: stars — stars: neutron

1. INTRODUCTION

A key issue in pulsar and black hole electrodynamics is the injection of plasma on open magnetic field lines. In the absence of adequate plasma, referred to as a “gap” where the system is said to be “charge-starved,” the rotation of the compact object induces a component of the electric field parallel to magnetic field lines, E_{\parallel} , which accelerates any test particle to a very high energy. Such “primary” particles reach energies at which the photons they emit, through curvature radiation (CR) or inverse Compton scattering (ICS), exceed the threshold for effective pair creation, leading to a pair cascade that populates the magnetosphere with “secondary” pairs. The charge-starved E_{\parallel} is screened once the pair plasma is sufficiently dense to provide the Goldreich-Julian (GJ) charge density. To maintain the electric charge density close to the GJ value, the charges must be injected continuously at an average rate equal to the escape rate of charged particles along open magnetic lines.

In a conventional class of pulsar models (e.g., the reviews by Michel 1991; Beskin et al. 1993; Mestel 1999), which we refer to as gap-plus-PFF (pair formation front) models, the system is assumed to be in a steady state in the corotating frame. The gap, the region of pair creation, and the region where E_{\parallel} is screened are assumed to be spatially separated. Charge starving in an “inner gap” near the stellar surface results in pair creation that is strongly concentrated in a narrow range of heights, referred to as a PFF or a pair production front. Reflecting secondaries (positrons if the primaries are electrons) provide a net quasi-static charge density, such that the PFF may be regarded as a thin surface with a surface charge density. The resulting additional electrostatic field screens out the initial E_{\parallel} above the PFF (e.g., Fawley et al. 1977; Arons & Scharlemann 1979; Shibata et al. 1998). In some pulsar models pairs are also assumed to be produced in an “outer gap” (Cheng et al. 1986), and current conservation can be achieved by the currents through the inner and outer gaps being part of a global circuit (Shibata 1991). More

recent models differ quantitatively, rather than qualitatively, from earlier models in that the Lorentz factors of the secondary pairs are smaller (Zhang & Harding 2000; Hibsman & Arons 2001; Arendt & Eilek 2002) and the pair creation is over a more extensive region, with the heights of the inner and outer gaps perhaps overlapping (Shibata et al. 2002). Despite extensive studies of such models, it remains unclear how and where the radio emission is generated. One observational estimate of the location of the source of the radio emission (Blaskiewicz et al. 1991; Gangadhara & Gupta 2001) suggests that it is between the putative inner and outer gaps. Although the possible high-energy emission processes are well understood, there is no consensus on the location of the high-energy emission region, with strong arguments for both the inner gap (Harding & Muslimov 1998) and the outer gap (Romani 1996). The lack of success of pulsar models in explaining the observed emissions (e.g., Beskin 1999) leaves open the possibility that one or more of the basic assumptions in the model may be incorrect. A critical review of the assumptions was given by Michel (2004), who favored a radically different model involving a large Coulomb field associated with charge-separated regions of the magnetosphere (Krause-Polstorff & Michel 1985).

In this paper we relax the steady state assumption, arguing that the stability of models involving steady state pair creation at a PFF is questionable. In fact, early models that did not make the steady state assumption predate later models that did. In particular, Sturrock (1971) argued that a steady state is not possible and that the pairs escape in a sequence of sheets. Ruderman & Sutherland (1975) invoked pair creation in bursts, called sparking (see also Beskin 1982). One specific difficulty with a steady state model relates to the reflection of secondaries at the PFF. Suppose that E_{\parallel} accelerates electrons upward, so that it accelerates secondary positrons downward. Steady state models that assume the screening of E_{\parallel} above the PFF to be sufficient to prevent reflection of secondary positrons (Shibata et al. 1998) require such implausibly large densities that they seem untenable. When trapped positrons are properly accounted for, a steady state solution can be obtained, under certain conditions, in which the number of reflected positrons is small and does not lead to a disruption of the primary electron beam (Arons & Scharlemann

¹ School of Physics and Astronomy, Tel Aviv University, Tel Aviv 69978, Israel; levinson@wise.tau.ac.il.

² School of Physics, University of Sydney, NSW 2006, Australia.

1979; Arons 1981). If a substantial fraction of the positrons are reflected, such positrons become downward-propagating counterparts of the primary electrons and by the same sequence of processes can, under some conditions, create a second PFF near the stellar surface (Harding & Muslimov 1998). Reflection of the created electrons at this second PFF may in turn greatly increase the number of primary electrons, leading to a rapidly increasing rate of pair creation. Such a runaway pair creation would not just short out the initial E_{\parallel} , but overshoot it, setting up oscillations with a large amplitude, of the order of the initial E_{\parallel} . Fine-tuning is required in order to have a sufficient number of reflected positrons to allow screening, but not too many to cause an overshoot setting up oscillations. This leads us to suspect that the steady state solutions are unstable. The question of stability was mentioned by Arons & Scharlemann (1979) and Muslimov & Harding (1997), but it is not possible to discuss the stability to temporal perturbations within the framework of a steady state model.

We emphasize that the stability of the PFF to oscillations cannot be explored within the framework of conventional gap-plus-PFF models. This is because the steady state assumption, which presupposes that any screening is independent of time, precludes any consideration of temporal perturbations. Temporal perturbations in the electric field and the current are related by the induction equation, which is specifically excluded by the steady state assumption. This raises the possibility of a qualitatively different type of model, one that is oscillatory and governed by inductive effects, rather than steady state and governed by electrostatic effects.

In this paper we formulate an alternative model in which E_{\parallel} is oscillatory, with an amplitude of the order of the unscreened E_{\parallel} . Although the electrodynamics in the oscillatory and steady state models is quite different (inductive vs. electrostatic effects), there is some correspondence between spatially localized phenomena in steady state gap-plus-PFF models and temporally localized phenomena in an oscillatory model. The inner gap is replaced by an initially charge-starved region that we also refer to as a gap. The spatially localized pair creation at a PFF in a steady state model is replaced by temporally localized bursts of pair creation, near the phases where $|E_{\parallel}|$ is at a maximum. The GJ charge density can be included through a small asymmetry in the oscillatory model. There is a steady state current (along a given magnetic flux tube) that is a free parameter in either type of model. However, by hypothesis there is no time-varying current in a steady state model, whereas the time-varying current is intimately related to the oscillating electric field through the induction equation in the oscillatory model.

The model is introduced in § 2, and numerical results for some illustrative cases are presented in § 3. The model is discussed further in § 4.

2. OSCILLATING PAIR-CREATING ELECTRIC FIELD

In a frame corotating with the star, Maxwell's equations can be written in the form

$$\nabla \cdot \mathbf{E} = 4\pi(\rho - \rho_{\text{GJ}}), \quad (1)$$

$$\nabla \cdot \mathbf{B} = 0, \quad (2)$$

$$\nabla \times \mathbf{E} = -\frac{1}{c} \frac{\partial \mathbf{B}}{\partial t}, \quad (3)$$

$$\nabla \times \mathbf{B} = \frac{4\pi}{c} (\mathbf{j} - \mathbf{j}_R) + \frac{1}{c} \frac{\partial \mathbf{E}}{\partial t}, \quad (4)$$

where ρ_{GJ} is the GJ charge density and the term \mathbf{j}_R is a combination of the fields and their derivatives and is given explicitly in Fawley et al. (1977). The electromagnetic fields, current density, and charge density are in the corotating frame. The electric current density is anticipated to be on the order of $c\rho_{\text{GJ}}$ or larger (this is also true in steady state situations). We then find $j_R/j \sim \Omega R/c \ll 1$, where R is radial distance, and can therefore neglect the term \mathbf{j}_R in equation (4) except near the light cylinder.

The model developed in this paper is one-dimensional, involving an electric field parallel to the magnetic field, as in steady state models. This involves ignoring drift motion (both inertial and $\mathbf{E} \times \mathbf{B}$) of charged particles, so that the motion of pairs is restricted to the direction along magnetic field lines. This is a good approximation well inside the light surface. We define s to be the distance along a magnetic field line and let the field-aligned (parallel) and cross-field (perpendicular) components of the electric field be E_{\parallel} and \mathbf{E}_{\perp} , respectively. The one-dimensional assumption implies the neglect of \mathbf{E}_{\perp} and that E_{\parallel} and ρ are functions only of s and t . The important difference in our model is that E_{\parallel} is determined by inductive effects, described by a time-varying (parallel) current in equation (4), whereas in the steady state model E_{\parallel} is determined by equation (1).

Before making the one-dimensional approximation, from equations (1)–(4) we obtain a wave equation for the electric field,

$$\nabla^2 \mathbf{E} - \frac{1}{c^2} \frac{\partial^2}{\partial t^2} \mathbf{E} = \frac{4\pi}{c^2} \frac{\partial \mathbf{j}}{\partial t} + \nabla(\rho - \rho_{\text{GJ}}), \quad (5)$$

and the equation of charge continuity, in the form $\partial(\rho - \rho_{\text{GJ}})/\partial t + \nabla \cdot \mathbf{j} = 0$. In the one-dimensional case, the equation of charge continuity continues to apply, but one has $\nabla \times \mathbf{E} = 0$, so that equation (3) is not relevant. The neglect of \mathbf{E}_{\perp} implies neglect of transverse oscillations, satisfying equation (5). The oscillations on which we concentrate satisfy the parallel component of equation (5).

In the one-dimensional case, equation (1) reduces to

$$\frac{\partial E_{\parallel}}{\partial s} = 4\pi(\rho_e - \rho_{\text{GJ}}). \quad (6)$$

Substituting equation (6) into equation (5) and integrating over time yields

$$\frac{\partial E_{\parallel}}{\partial t} = -4\pi(j_{\parallel} - j_0), \quad (7)$$

where j_0 is a constant of integration. Equations (6) and (7) are related by the equation of charge continuity. Using equation (4), we obtain $j_0 = \mathbf{b} \cdot (\nabla \times \mathbf{B})$, where \mathbf{b} is a unit vector along the magnetic field. Our neglect of variations across magnetic field lines implies in addition $\partial j_0/\partial s = 0$. The constant j_0 is a free parameter in our model, associated with the global direct current flowing along the corresponding magnetic field line. Using $\nabla \cdot \mathbf{j} + \partial \rho_e/\partial t = 0$ and the fact that j_0 is divergence free, we obtain

$$\frac{\partial}{\partial t} \left(\frac{\partial E_{\parallel}}{\partial s} - 4\pi \rho_e \right) = 0. \quad (8)$$

Consequently, Poisson's equation in the form of equation (6) is automatically satisfied and is needed only to determine the initial electric field $E_{\parallel}(t=0, s)$ for a given choice of initial charge distribution. As a check of our calculations, we verify

that equation (6) is satisfied every several time steps during each run.

In steady state models $j_{\parallel} = j_0$ is implicit at all times, so that $\partial E_{\parallel}/\partial t = 0$. Equation (6) is then solved together with the equation of motion for the accelerating pairs, and some prescription for pair creation is adopted. In most cases it has been shown that for reasonable pair multiplicities (number of secondary pairs per primary particle) the model predicts some returning positrons, which are usually ignored. However, any change in the number of returning positrons, as necessarily occurs in any perturbation away from the steady state, implies a change in the current density inside the gap from the assumed value j_0 . To treat such an effect requires use of equation (7), and this equation is excluded by the steady state assumption. According to equation (7), any non-zero difference $j_{\parallel} - j_0$ leads to a temporally varying E_{\parallel} . For a steady state model to be stable, the resulting varying E_{\parallel} must eventually be damped so that the steady state is restored. However, pair creation should lead to an increase in $|j_{\parallel} - j_0|$, until the system overshoots, leading to oscillations in E_{\parallel} . Moreover, it is not at all clear that for arbitrary initial conditions the pair cascade process can relax to the putative steady state. Below, we demonstrate that indeed a plausible mode of operation is large-amplitude oscillations that control the pair creation rate via a positive feedback, with no indication that the oscillations damp and hence no indication that the system converges to a steady state.

We adopt a treatment in which the plasma is modeled as a two-component fluid, consisting of electrons and positrons. We introduce the equations in a covariant formalism (Greek indices run over 0, 1, 2, and 3, with the signature of the metric +2) and then revert to the one-dimensional (along the parallel axis) form for our specific calculations. The processes incorporated in the model are emission of CR photons and one-photon creation of e^{\pm} pairs on the external magnetic field.

Let

$$T_{\pm}^{\alpha\beta} = h_{\pm} n_{\pm} U_{\pm}^{\alpha} U_{\pm}^{\beta} + p_{\pm} g^{\alpha\beta} \quad (9)$$

denote the stress energy tensor of electrons (minus) and positrons (plus), where n_{\pm} , U_{\pm}^{α} , p_{\pm} , and h_{\pm} are their proper density, 4-velocity, partial pressure, and specific enthalpy, respectively, and let $Q/2$ denote the total creation rate per unit volume of electrons (or positrons). The continuity equations are

$$\partial_{\alpha}(n_{\pm} U_{\pm}^{\alpha}) = Q/2. \quad (10)$$

The energy and momentum equations can be expressed as

$$\partial_{\alpha}(T_{\pm}^{\alpha\beta}) = \pm en_{\pm} F^{\beta}_{\alpha} U_{\pm}^{\alpha} - S_{\pm}^{\beta} + Q_{\pm}^{\beta}, \quad (11)$$

where $F^{\alpha\beta} = -F^{\beta\alpha}$ is the Maxwell 4-tensor. The terms S_{\pm}^{β} and Q_{\pm}^{β} account, respectively, for radiative losses due to the emission of CR photons and the change in energy and momentum of the pairs due to pair creation.

The 4-current density is given by

$$j^{\mu} = e(n_{+} U_{+}^{\mu} - n_{-} U_{-}^{\mu}). \quad (12)$$

The charge conservation relation $\partial_{\mu} j^{\mu} = 0$ is implied by equation (10).

The projection of equation (11) on the 4-velocity U^{β} yields an equation for the change of specific entropy, σ_{\pm} , of each fluid,

$$n_{\pm} T_{\pm} U_{\pm}^{\alpha} \partial_{\alpha} \sigma_{\pm} = S_{\pm}^{\beta} U_{\pm\beta} - Q_{\pm}^{\beta} U_{\pm\beta} - h_{\pm} Q/2, \quad (13)$$

where T_{\pm} are the corresponding temperatures. The first term on the right-hand side of equation (13) accounts for the decrease in specific entropy due to radiative losses, and the last two terms account for the change in the specific entropy resulting from conversion of photons to pairs.

Using equations (9), (10), (11), and (13), we obtain the equation of motion of each fluid,

$$n_{\pm} h_{\pm} U_{\pm}^{\alpha} \partial_{\alpha} U_{\pm}^{\beta} = \pm en_{\pm} F^{\beta}_{\alpha} U_{\pm}^{\alpha} + (-S_{\pm}^{\alpha} + Q_{\pm}^{\alpha}) \Theta_{\pm\alpha}^{\beta} - \Theta_{\pm}^{\alpha\beta} \partial_{\alpha} p_{\pm}, \quad (14)$$

where $\Theta_{\pm}^{\alpha\beta} = g^{\alpha\beta} + U_{\pm}^{\alpha} U_{\pm}^{\beta}$.

In order to solve the set of equations, we need to make a number of simplifying assumptions, and in doing so we seek the simplest possible model that retains the features that we consider essential.

We make the following simplifications. First, under the conditions considered below we anticipate the pressure forces to be much smaller than the electric force. We therefore neglect the last term on the right-hand side of equation (14). Second, we suppose that the specific entropy of each fluid is roughly conserved along streamlines, that is, we take $U_{\pm}^{\alpha} \partial_{\alpha} \sigma_{\pm} = 0$ in equation (13). We emphasize that intense pair creation does not necessarily imply that the entropy per particle must increase. The average energy of CR photons is much smaller than the energy of radiating pairs, so that any change in the specific entropy during a burst of pair creation should be sufficiently small not to affect the general conclusions drawn below. Third, we ignore any $\mathbf{E} \times \mathbf{B}$ drift and consider only acceleration along magnetic field lines. Fourth, we adopt simple models for the source terms S_{\pm}^{β} and Q_{\pm}^{β} that are intended to model the effects of CR; we ignore ICS, which is more difficult to model. Fifth, we do not include escape of particles explicitly. This is an obvious weakness in the model, because escape of particles to form the pulsar wind is an essential aspect of pulsar physics. Moreover, particles can escape to the stellar surface, heating it and possibly leading to observable X-ray emission. However, in the simplest version of the model here we concentrate on the creation of the pairs within the gap region.

We adopt a local coordinate frame in which $F^1_0 = E_{\parallel}$. We denote by $U \equiv U^1$ the component of the 4-velocity along the magnetic field, by v the corresponding 3-velocity, by $N_{\pm} = n_{\pm} \Gamma_{\pm}$ the pair density as measured in the laboratory frame, and by $s_{\pm}^1 = S_{\pm}^1/N_{\pm}$, $q_{\pm}^1 = Q_{\pm}^1/N_{\pm}$, and $q_{\pm} = Q/2N_{\pm}$ the radiative drag per particle, momentum gain per particle due to photon conversion, and pair multiplicity rate, respectively. Under the above assumptions equations (14) and (10) reduce to

$$\frac{\partial U_{\pm}}{\partial t} + v_{\pm} \frac{\partial U_{\pm}}{\partial s} = \pm \frac{e E_{\parallel} c^2}{h_{\pm}} - \frac{s_{\pm}^1}{h_{\pm}} + \frac{q_{\pm}^1}{h_{\pm}} - q_{\pm} U_{\pm}, \quad (15)$$

$$\frac{\partial N_{\pm}}{\partial t} + \frac{\partial}{\partial s}(N_{\pm} v_{\pm}) = Q/2. \quad (16)$$

The enthalpies h_{\pm} are free parameters in the model (they are assumed to be time independent). The maximum Lorentz factor, γ_{\max} , that a test particle can acquire during the initial pair creation burst is limited by radiative drag. To estimate γ_{\max} during the pair creation burst, we equate the electric force with the CR loss per unit length to obtain $\gamma_{\max} \simeq 2 \times 10^5 E_{\parallel}^{1/4}$. For a pulsar having $B \leq B_c$, where $B_c = m_e^2 c^3 / e \hbar^2$ is the critical field strength, the vacuum electric field near the surface is $E_s \sim \Omega_s B_s R_s \leq 5 \times 10^8 \text{ V cm}^{-1}$, yielding $\gamma_{\max} < 10^7$. This implies that

the characteristic energy of CR photons is $\epsilon_{\gamma\pm} = 1.5\gamma_{\max}^3 \hbar c / \rho_B < 10^5 m_e c^2$, where $\rho_B \gtrsim R_s$ is the radius of curvature of the magnetic field lines along which the pairs are accelerated. Hence, the energy of newly created pairs is much smaller than the maximum energy $m_e c^2 \gamma_{\max}$. Consequently, the fraction of pairs having the maximum Lorentz factor is expected to be small during a burst of pair creation. Indeed, as shown below, during a burst of pair creation the average Lorentz factor is determined by mass loading and is typically well below γ_{\max} . The amplitude of oscillations of the 4-velocity decreases as the pair density increases, due to mass loading (the energy in the oscillations is redistributed to a larger number of pairs), until it reaches a value at which the energy of CR photons equals the threshold for a single photon annihilation, at which point pair creation ceases.

A detailed derivation of the energy distribution of pairs involves solving the relevant kinetic equations, and a simpler approach is needed for the present purpose. We assume that the spread in Lorentz factors of particles in each fluid is small with respect to the bulk Lorentz factor and take the energy-loss term to be $s_{\pm}^0 = 2e^2 c \Gamma_{\pm}^4 / 3\rho_B^2$ for CR, where Γ_{-} (Γ_{+}) is the bulk Lorentz factor of the electron (positron) fluid. Under the reasonable assumption that the particles in each fluid are distributed isotropically in the fluid rest frame, we obtain

$$s_{\pm}^1 = s_{\pm}^0 v_{\pm} = \frac{2e^2 c \Gamma_{\pm}^3 U_{\pm}}{3\rho_B^2}. \quad (17)$$

The characteristic energy of a CR photon is $\epsilon_{\gamma\pm} = 1.5\Gamma_{\pm}^3 \hbar c / \rho_B \simeq 10^{-10.5} \Gamma_{\pm}^3 (\rho_B / 10^6 \text{ cm}) \text{ eV}$. Provided the energy of the emitted photon satisfies $\epsilon_{\gamma} \sin \psi > 2m_e c^2$, where ψ is the angle between the photon momentum and the direction of the local magnetic field, the photon can decay into an electron-positron pair. The lifetime for this decay is assumed to be short: all photons are assumed to decay instantaneously once the energy of the particle emitting the CR photons exceeds an effective threshold value, Γ_{thr} . The number of photons of characteristic energy produced per unit time per unit volume by the electron fluid is approximately $d^2 N_{\gamma} / dt dV \sim N_{-} s_{-}^0 / \epsilon_{\gamma_{-}} \simeq 10^2 N_{-} \Gamma_{-}$, and likewise for the positron fluid. These photons are converted into pairs over a distance $\Delta s \ll \rho_B$ if $\Gamma_{\pm} \gg \Gamma_{\text{thr}}$. Thus, the source terms associated with pair creation can be approximated as

$$Q = \alpha_{+} N_{+} + \alpha_{-} N_{-}, \quad (18)$$

$$q_{\pm}^1 = (\alpha_{+} N_{+} \epsilon_{\gamma_{+}} + \alpha_{-} N_{-} \epsilon_{\gamma_{-}}) c / 2N_{\pm}, \quad (19)$$

where $\alpha_{\pm} = 10^2 \Gamma_{\pm}$ for $\Gamma_{\pm} > \Gamma_{\text{thr}}$ and $\alpha_{\pm} = 0$ otherwise. The threshold value above which CR photons annihilate inside the gap is a function of position, but for simplicity we take it to be a fixed value (except for one example, as explained below), which is a free parameter in our model. The value we adopt in our calculations is $\Gamma_{\text{thr}} = 10^6$.

Once pairs are accelerated to Lorentz factors in excess of Γ_{thr} , the pair density rises rapidly. The bulk Lorentz factor grows until the right-hand side of equation (15) vanishes, at which point it saturates. Using equations (17) and (19), we find that this happens roughly when $eE_{\parallel} c^2 = h_{\pm} q_{\pm} U_{\pm}$. When the pair system becomes roughly symmetric, the Lorentz factors of the fluids saturate at a value given by

$$\Gamma_{+} = \Gamma_{-} \simeq 10^4 \tilde{E}_{\parallel}^{1/2}, \quad (20)$$

where \tilde{E}_{\parallel} is defined below. Our interpretation is that the bulk Lorentz factors are limited by mass loading. Specifically, as the bulk Lorentz factors of the accelerating fluids approach this value, the pair creation rate increases to a level at which the electric potential energy goes to create additional pairs that move at the same bulk Lorentz factor, rather than accelerating the fluids.

The above equations can be rendered dimensionless by employing the normalization $\tilde{E} = eLE/m_e c^2$, $\tilde{N} = N/N_B$, and $\tilde{j}_0 = j_0/(eN_B c)$ and measuring velocities in units of c , distances in units of L , and time in units of ω_B^{-1} . Here $N_B = \Omega_s B_s / 2\pi e c$, $\omega_B^2 = 4\pi e^2 N_B / m_e$, and $L = c/\omega_B$, where B_s is the magnetic field strength at the stellar surface and $\Omega_s = 2\pi P$ is the angular velocity of the star. Note that in these units the vacuum electric field near the surface is given as

$$\begin{aligned} \tilde{E}_s &= eL\Omega_s B_s R_s / m_e c^3 \\ &= 3 \times 10^6 (B_s / B_c)^{1/2} (P / 1 \text{ s}^{-1})^{1/2} (R_s / 10^6 \text{ cm}). \end{aligned} \quad (21)$$

In what follows we use this normalization with $B_s = B_c$, $R_s = 10^6 \text{ cm}$, and $P = 1 \text{ s}^{-1}$.

3. RESULTS

To obtain our numerical results, we integrated equations (7), (12), (15), (16), (17), (18), and (19) on a uniform computational grid with 10^4 cells. In all the examples presented below the inner boundary is at the stellar surface, and the outer boundary is above the pair creation region. The boundary condition imposed at the outer boundary of the computational domain is the zero-gradient condition, which minimizes the effect of the boundary condition on the solution. We made some runs with other boundary conditions and found little difference in most cases.

In the first example that we considered we made the simplest assumptions to illustrate the essential features of the model. In this model all quantities are assumed to be initially homogeneous within the gap, and the pair creation rate is also homogeneous with a threshold $\Gamma_{\text{thr}} = 10^6$. This is intended to model sparking in a region close to a charge-starved stellar surface. It is readily seen that under these conditions the system remains homogeneous at all times, so that the variations are purely temporal. An example is shown in Figure 1, where the electric field [normalized to the initial value $E_0 = E_{\parallel}(t=0)$] and 4-velocity, normalized to the threshold Lorentz factor ($\Gamma_{\text{thr}} = 10^6$ in this example), are plotted against dimensionless time, for two different initial conditions. The top two panels correspond to initial electric field $\tilde{E}_0 = -10^4$, and the bottom panels to $\tilde{E}_0 = -10^6$. The evolution of the corresponding electron density is exhibited in Figure 2; the positron density equals the electron density. The initial pair densities in both cases were taken to be $\tilde{N}_{\pm} = 10^{-2}$, and the initial velocities were $U_{-} = 0.95$ and $U_{+} = 0$. The parameter j_0 was set equal to the initial current density, viz., $j_0 = j_{\parallel}(t=0) = -6.9 \times 10^{-3} N_B c$. We assumed cold fluids: $h_{\pm} = m_e c^2$.

As clearly seen from Figure 1, the 4-velocity increases rapidly initially until it reaches the value given by equation (20), at which point a burst of pair creation commences, as can be seen from Figure 2. This is followed by a phase during which the pair density and hence the electric current density j_{\parallel} rise exponentially while the bulk velocity remains approximately constant. As j_{\parallel} grows, the rate of change of the electric field, given by equation (7), increases. The electric field eventually passes through zero and reverses sign, leading to a deceleration

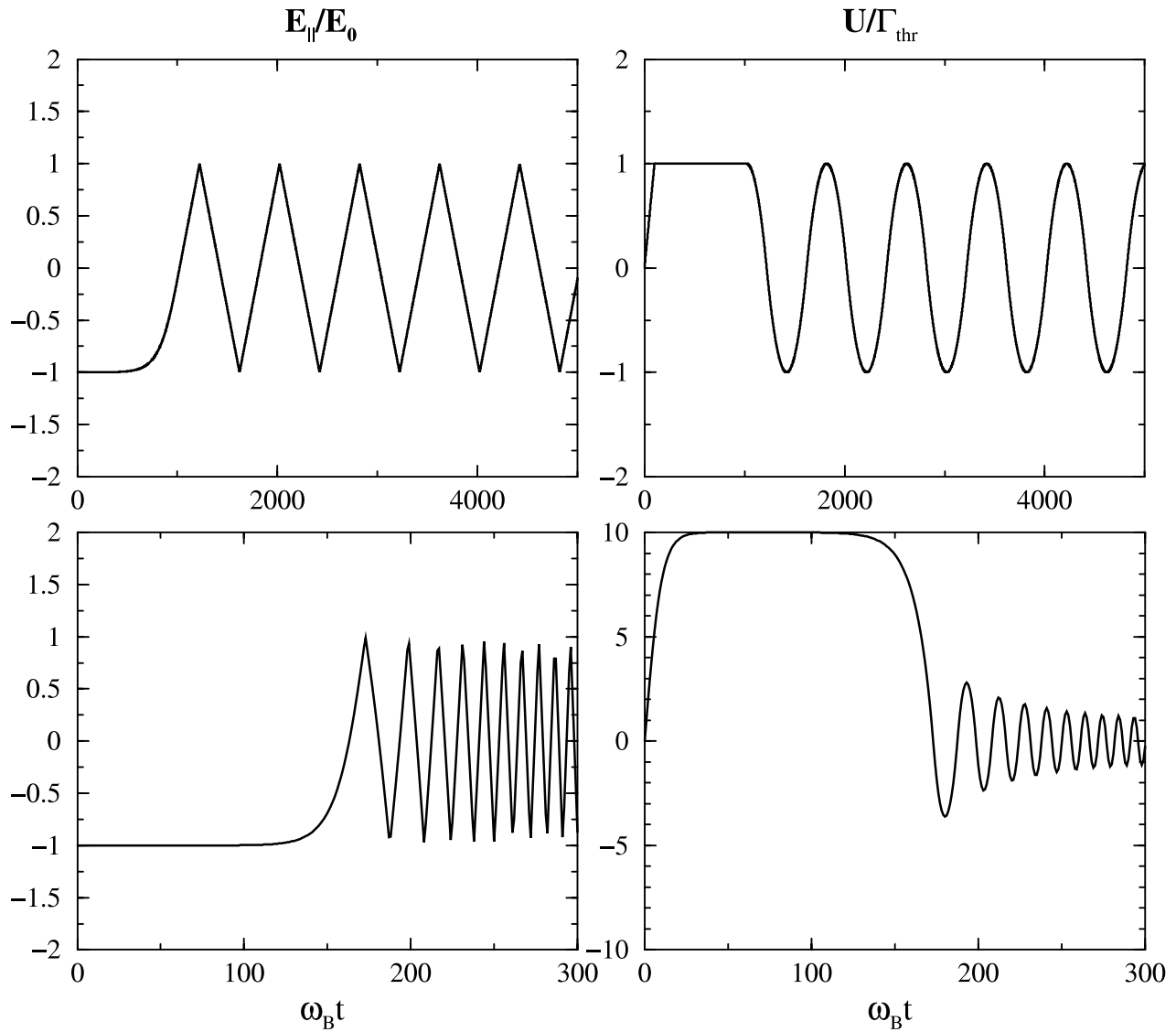


FIG. 1.—Evolution of the E_{\parallel} (left panels) and the 4-velocity (right panels) in a large-amplitude oscillation with a uniform initial electric field $\tilde{E}_0 = -10^4$ (top panels) and $\tilde{E}_0 = -10^6$ (bottom panels). The 4-velocity saturates at $U/\Gamma_{\text{thr}} = 1$, below which pair creation becomes ineffective, and the system oscillates after the charge screening overshoots.

of the bulk flow. The system then continues to oscillate. As seen from Figure 1, the amplitude of oscillations of the 4-velocity damps over several periods until it reaches the pair creation threshold, Γ_{thr} , at which point the pair cascade process terminates abruptly.

The sawtooth shape of the electric field oscillations is a consequence of a relativistic effect. The electric current density is proportional to the 3-velocity of the charged particles, which is approximately constant at $\pm c$ during each cycle, except for a short period during which the particles become nonrelativistic briefly and the current density changes sign abruptly. To see this more clearly, consider the oscillations after the pair creation burst ceases and the pair density saturates. Then $N_+ \simeq N_- = N_0$ is independent of time, and so $j_{\parallel} = e(N_+ v_+ - N_- v_-) \simeq 2eN_0 v_-$ is also time independent as long as $U_{\pm} \gg 1$. Equation (7) then implies that E_{\parallel} changes linearly with time during most of the oscillation period. Specifically,

$$E_{\parallel} \approx E_0 \begin{cases} t/T_- & \text{for } -T_- < t < T_-, \\ (T_- + T_+ - t)/T_+ & \text{for } T_- < t < T_- + 2T_+, \end{cases} \quad (22)$$

where $T_{\pm} = \omega_B^{-1} \tilde{E}_0 / (\tilde{N} \pm \tilde{j}_0)$, with \tilde{E}_0 as the amplitude of the electric field oscillations, roughly equal to the strength of the initial field, and $\tilde{N} = \tilde{N}_+ = \tilde{N}_-$. The sign change of the electric current occurs over a fraction $\Gamma_{\text{thr}}^{-1/2}$ of the period. When $j_0 \neq 0$ the oscillations are asymmetric in time. In the example shown in Figure 1, where j_0 is negative, the time it takes the electric field to change from $\tilde{E}_{\parallel} = -\tilde{E}_0$ to $\tilde{E}_{\parallel} = +\tilde{E}_0$ is slightly longer than the time it takes it to change back. As a consequence, the time-averaged 4-velocities, $\langle U_- \rangle$ and $\langle U_+ \rangle$, do not vanish, as in the case of symmetric oscillations. In fact, equations (7), (12), and (15) imply $ec(N_+ \langle U_+ \rangle - N_- \langle U_- \rangle) = j_0$, as expected. This asymmetry is small in this example, where the direct current j_0 is much smaller than the oscillating current j_{\parallel} and is not well resolved in Figure 1. By employing equations (7) and (12) and ignoring this small asymmetry, we estimate the oscillation period of the saturated system (after pair creation effectively ceases) to be $T = \omega_B^{-1} (4\tilde{E}_0/\tilde{N})$. Integrating equation (15) from $U = 0$ to $U = U_{\text{max}}$, using the above result for the period T , and taking the amplitude of the 4-velocity oscillations to be $U_{\text{max}} \simeq \Gamma_{\text{thr}}$ yields the saturated pair density in terms

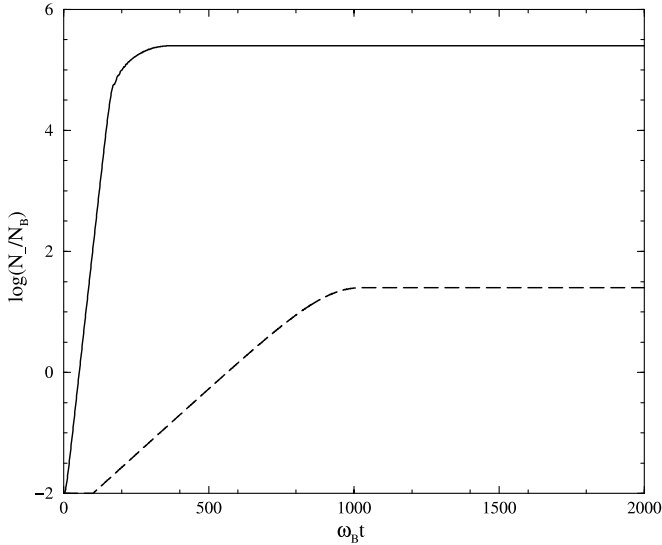


FIG. 2.—Evolution of the pair density, showing an exponential increase until the screening overshoots, after which it remains roughly constant as the system oscillates. The dashed line corresponds to the case with $\tilde{E}_0 = -10^4$ in Fig. 1, and the solid line to $\tilde{E}_0 = -10^6$.

of the initial electric field strength and the threshold Lorentz factor,

$$N \simeq N_B \frac{\tilde{E}_0^2}{2\Gamma_{\text{thr}}} = \frac{E_0^2}{8\pi m_e c^2 \Gamma_{\text{thr}}}. \quad (23)$$

Substituting the last equation into the above expression for the oscillation period, we obtain

$$T = \omega_B^{-1} \frac{8\Gamma_{\text{thr}}}{\tilde{E}_0} = \frac{8m_e c}{eE_0} \Gamma_{\text{thr}}. \quad (24)$$

We find these analytic estimates to be in excellent agreement with the numerical results. Note that there is a positive feedback on the system; any loss of plasma from the gap, as expected in more realistic situations in which the gap is finite, would result in a reduction of the pair density \tilde{N} and a consequent increase of U_{max} . This would lead to regeneration of plasma inside the gap to compensate for the losses. The average pair creation rate would then be equal to the loss rate.

As a second example, we take the initial electric field to be the vacuum field of an aligned rotator near the axis. The vacuum field decreases with height above the stellar surface, and we

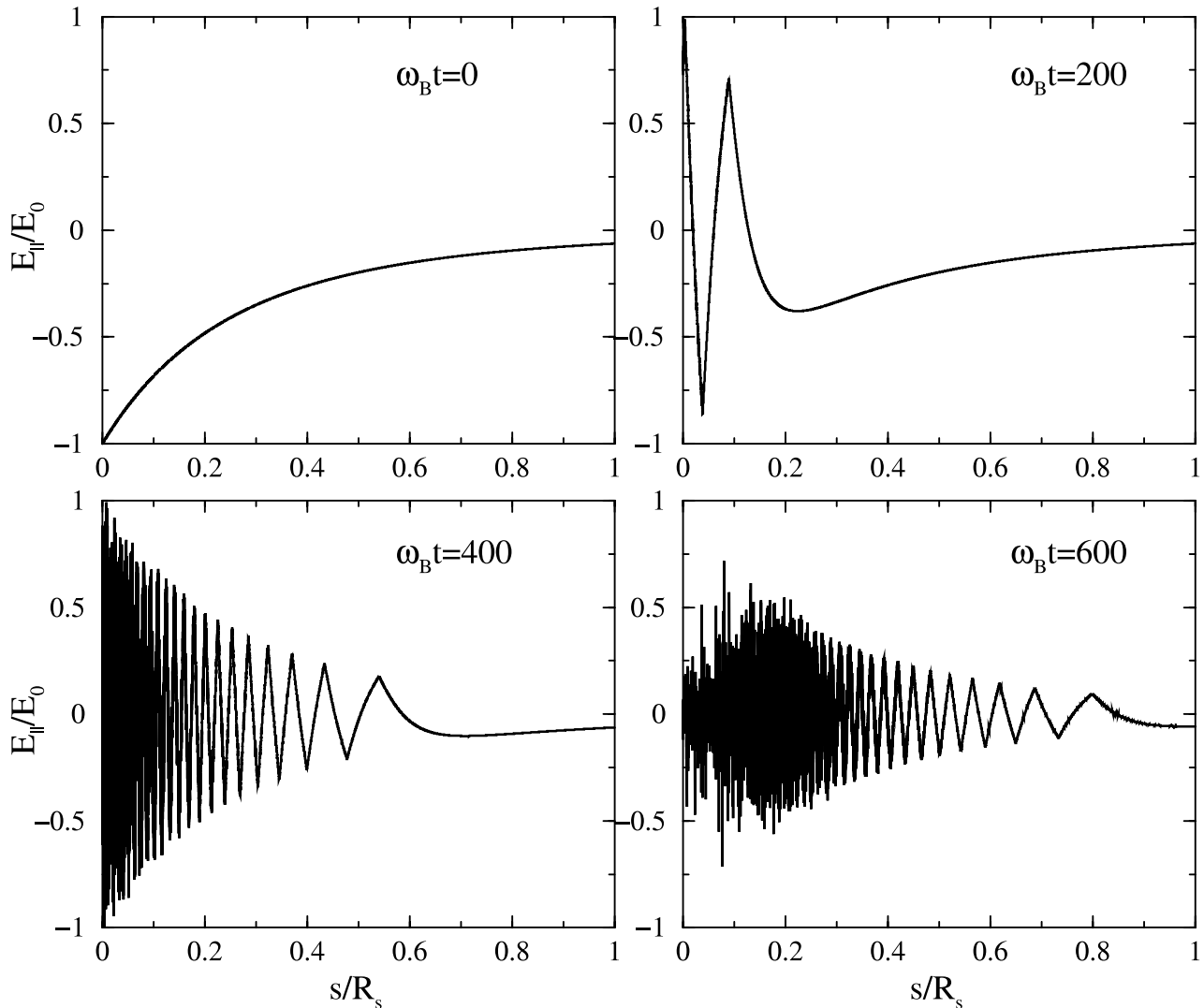


FIG. 3.—Evolution of the system starting from a charge-starved condition, with the vacuum electric field decreasing as illustrated in the top left panel. As time increases, oscillations are set up with their frequency and amplitude decreasing with height, as shown.

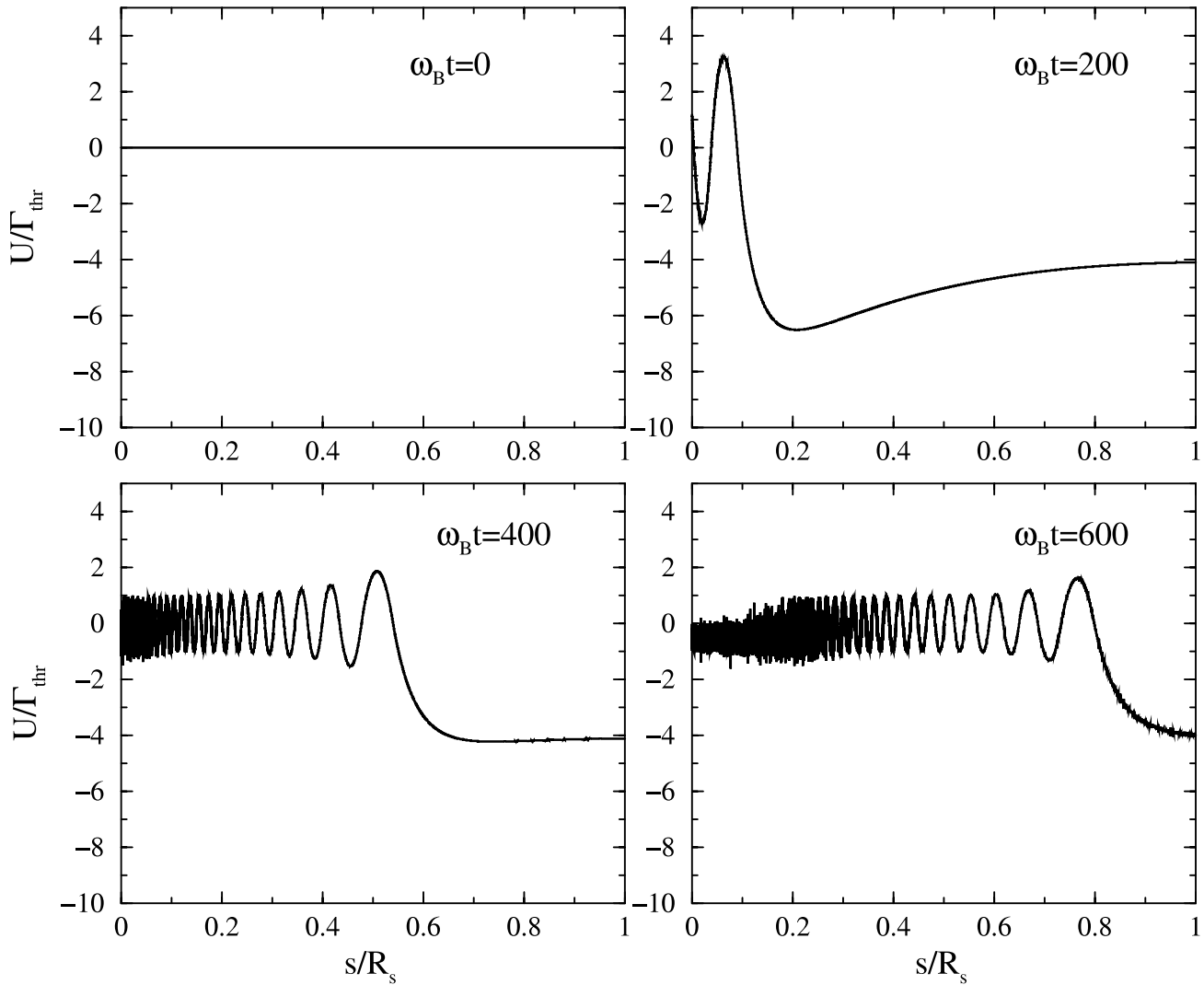


FIG. 4.—Evolution of the 4-velocity, for the same conditions as in Fig. 3.

take this spatial variation into account by adopting a simple model for it. To be more specific, we take $\tilde{E}_{\parallel}(s, t = 0) = \tilde{E}_s(1 + s/R_s)^{-4}$, with \tilde{E}_s given by equation (21). Because the magnetic field declines with height (increasing r), the absorption length of a single photon at a given energy increases with height in a manner that depends on the geometry of the magnetic field. For illustration, we take the source terms Q and q^1 as in equations (18) and (19), but with $\alpha_{\pm} = 10^2 \Gamma_{\pm} \exp[-(s/R_s)^2]$ if $\Gamma_{\pm} > \Gamma_{\text{thr}}$ and $\alpha_{\pm} = 0$ otherwise. In the cases shown in Figures 3–5, the initial pair density is $\tilde{N}_{+}(s, t = 0) = \tilde{N}_{-}(s, t = 0) = 10^{-2}$ for $s \leq R_s$ and zero for $s > R_s$, such that initial charge density is $\rho_e(s, t = 0) = e(N_{+} - N_{-}) = 0$. The initial 4-velocities were chosen such that the initial electric current density is equal to j_0 . We found that the final results are insensitive to the choice of the initial densities and velocities of electrons and positrons, provided they are much smaller than the final values. The evolution of the electric field is shown in Figure 3, where the electric field is plotted as a function of distance from the surface (located at $s = 0$). As seen from this time sequence, a wavelike pattern is formed above the surface and propagates outward. This is a consequence of the inhomogeneity of the system; since, as discussed above, the frequency of saturated parallel oscillations T^{-1} is roughly proportional to the local electric field strength

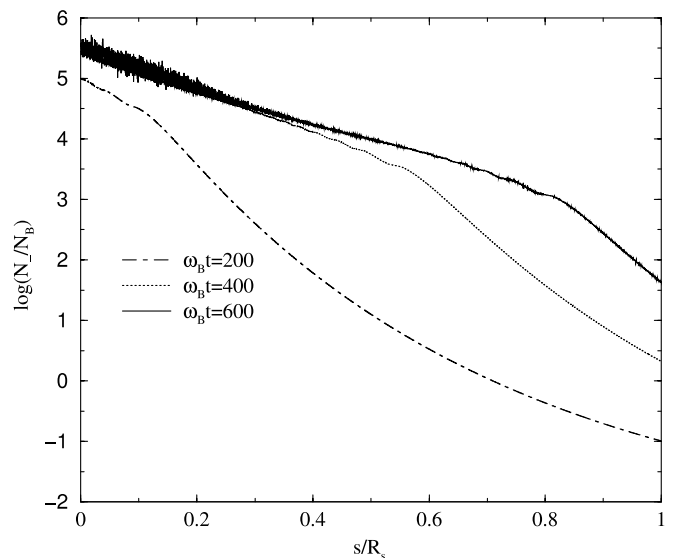


FIG. 5.—Density profile at three different times, computed for the same conditions as in Fig. 3.

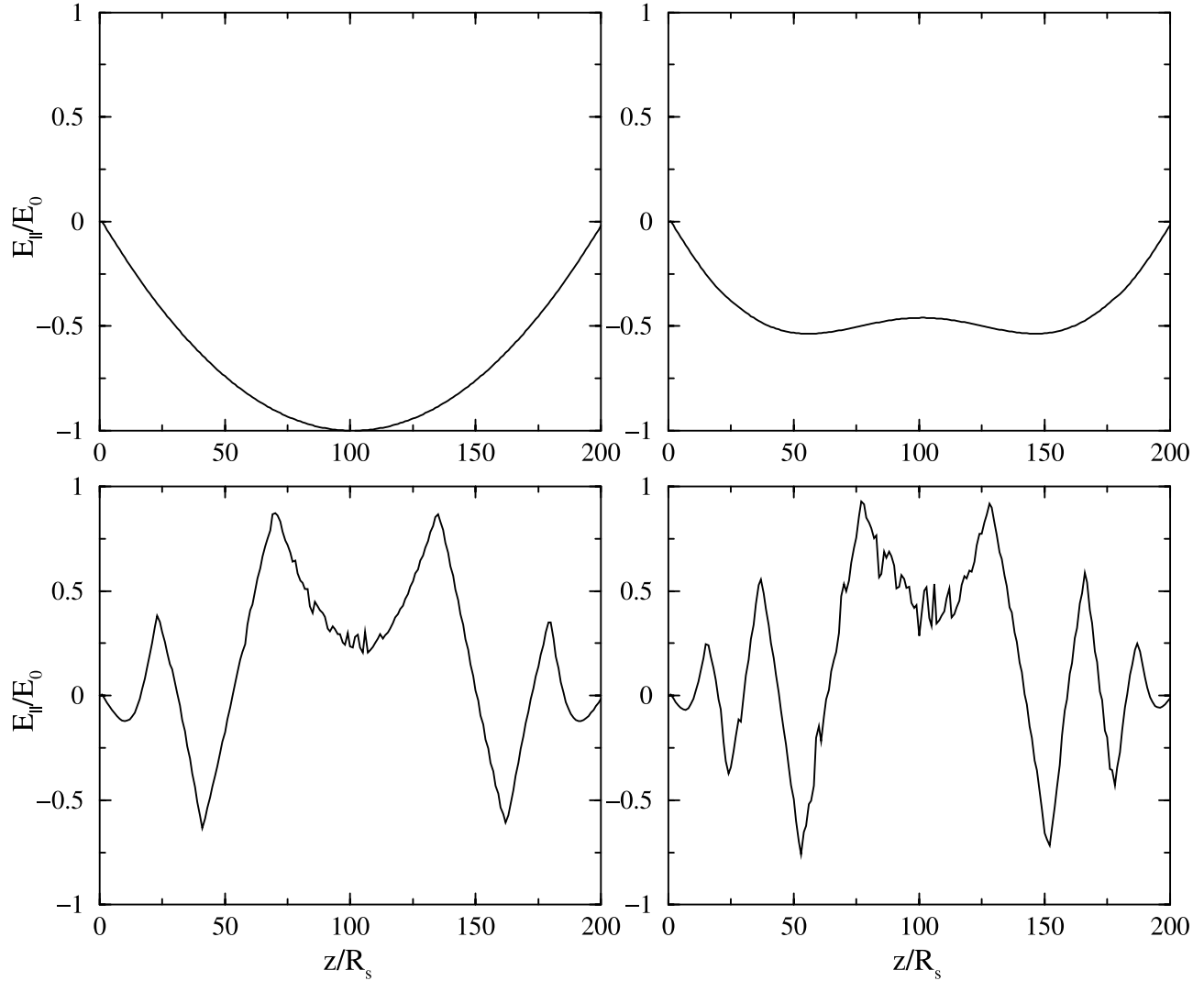


FIG. 6.—Evolution of the system starting from a parabolic parallel electric field, as shown in the top left panel.

$E_{\parallel}(s, t = 0)$, regions closer to the stellar surface, where the electric field is stronger, oscillate faster, as clearly seen in Figure 3. The corresponding 4-velocity is displayed in Figure 4: the amplitude approaches the (local) threshold value Γ_{thr} , as in the first example. The amplitude of the electric field oscillations near the surface becomes smaller with time. At $\omega_B t = 600$ the electric charge density reduces by a factor of about 10^2 relative to its value at $\omega_B t = 400$, although the pair density does not change much (see Fig. 5). As seen from Figure 4, at $\omega_B t = 600$ the oscillations of 4-velocity near the stellar surface become asymmetric, and it appears that both types of charge are convected toward the surface, although we emphasize that at this stage a better resolution is needed to resolve the structure near the surface.

Unfortunately, our numerical resolution is insufficient to follow the system for times longer than those shown, and it is not clear what the system evolves toward after a very long time. There is an indication in our calculations that after a sufficiently long time the system becomes chaotic. Physically, we expect that after pair creation effectively ceases, the rate of pair creation falls below the replacement rate needed to overcome escape of pairs, the oscillations break up, and a charge-starved configuration is reestablished. The evolution described above then repeats. However, we cannot confirm this expectation

within the framework of the present model, which does not include the escape of particles explicitly.

In our final example, we take the initial gap structure to be as in the model considered by Shibata et al. (1998). To be more precise, the initial electric field is given by $\tilde{E}_{\parallel}(s, t = 0) = s(1 - s/s_0)$ for $s \leq s_0$ and $E_{\parallel} = 0$ for $s > s_0$ (see Fig. 6). In the example shown in Figure 6, $s_0 = 0.05R_s$. For this choice of parameters the initial electric field is much smaller than the vacuum field given by equation (21), but still large enough to accelerate pairs well above Γ_{thr} . Since $s_0 \ll R_s$, the variation of the magnetic field is expected to be rather small, and we can therefore model pair creation using equation (19), with $\alpha_{\pm}/\Gamma_{\pm} = 10^6$ independent of radius. We find similar results as in the previous examples. Oscillations are set up locally inside the gap, and a wavelike pattern develops with time by virtue of the non-uniformity of the initial conditions. As seen, the electric field at the gap boundaries remains very small throughout the evolution of the system. The pair density near the boundaries is maintained roughly at the initial value. Pair creation is confined to the center of the gap, where the electric field strength is largest and can accelerate pairs to well above the pair creation threshold. Again, we are unable to follow the system for times longer than those shown. We anticipate that over very long timescales pairs will diffuse through the boundaries, owing to

relativistic and dispersion effects that should give rise to a finite group velocity.

4. DISCUSSION AND CONCLUSIONS

The preliminary calculations described in § 3 demonstrate that pair creation in pulsar and black hole magnetospheres is likely to be strongly oscillatory in nature rather than in a steady state. The essential difference between the oscillatory model proposed here and a steady state model is in the nature of the response to the E_{\parallel} that unavoidably develops in a pulsar magnetosphere. In an oscillatory model, this response is essentially inductive, intimately coupled to an oscillating current through the induction equation. In a steady state model E_{\parallel} is essentially electrostatic, and the induction equation is irrelevant by hypothesis. Our analysis shows that a partially unscreened E_{\parallel} tends to develop large-amplitude oscillations whenever the electric current deviates locally from the global direct current flowing in the system. Such deviations seem unavoidable in realistic situations. This suggests to us that steady state models are unstable to temporal perturbations and that the natural state of pair production in a pulsar magnetosphere is oscillatory. We emphasize that the stability of steady state models to temporal perturbations cannot be discussed within the framework of such models. Although we focus on pulsars here, we also expect similar behavior in magnetospheres of Kerr black holes.

Our results show that given an initial charge-starved configuration, the oscillations start with a brief episode during which the pair density rises exponentially, resulting from copious pair creation at phases of the oscillation around the maximum values of $|U_{\pm}|$. The resulting charge (and mass) loading of the oscillating system causes an increase in the frequency of oscillations (at a fixed height) and a decrease in the amplitude of the oscillations in the Lorentz factor. The pair density saturates when the maximum Lorentz factor decreases (due to mass loading) to the threshold for pair creation. The subsequent oscillations are maintained essentially at the threshold level, with a small net creation rate of pairs to balance losses due to escape. However, the limitations of the model, in the simplest form, preclude explicit treatment of escape. The oscillations in the saturated state are relatively stable, due to a positive feedback whereby any reduction in the pair density leads to an increase in the Lorentz factor of oscillating pairs and hence to an increase in the pair creation rate. The saturated pair density and corresponding frequency of oscillations depend only on the initial value of the parallel electric field and the threshold Lorentz factor for pair creation.

In situations where the initial state is not spatially uniform, the frequency of oscillations varies with position in the gap. Our calculations show a wavelike pattern developing in the inhomogeneous case, and it appears that the wavelike oscillations propagate to regions outside the gap. Our limited resolution does not allow us to follow the evolution of the system for a sufficiently long time (many light crossing times) to examine how the oscillations are transmitted to distant regions.

We regard the calculations presented in this paper as providing a basis for an alternative oscillatory model to the gap-plus-PFF model for the electrodynamics of pulsar magnetospheres. We make a number of major simplifications that need to be relaxed in a more realistic model, but we expect the main features identified here to remain in more realistic models. We comment specifically on three of our simplifying assumptions. First, the global direct current is a free parameter in our model, and the average charge density is determined from initial conditions. This means that the global structure of the magnetosphere is

not addressed within the framework of our analysis, only the microphysics of charge-starved regions. Second, we model the pair creation in a highly idealistic way: pairs are created only by particles above a specified threshold Γ_{thr} , and the pair creation is assumed to be instantaneous. This crude approximation should be adequate to describe the effects of an initial burst of pair creation starting from a charge-starved configuration, but more accurate approximations are needed to describe the effects of ongoing pair creation once the amplitude of the oscillations approaches a steady state. In addition, the simplified model of pair creation is derived assuming that the photons are due to CR, and we do not claim that it is realistic for resonant ICS (Sturmer 1995; Luo 1996), which is thought to dominate in some pulsars (Harding & Muslimov 1998). Third, our assumption that there is no spread in Lorentz factors (the electrons and positrons are cold in their respective instantaneous rest frames) may not be justified; in particular, the spread in Lorentz factors associated with the newly created pairs is comparable to the maximum Lorentz factor due to the oscillating electric field. This is particularly relevant in the early phase, when a burst of pair creation occurs. Furthermore, our neglect of the initial velocity of newly created pairs during the initial burst is justified only in the case of sufficiently strong electric fields, for which the acceleration length is much smaller than the characteristic size of the system. The inclusion of such effects requires the use of kinetic theory, and this greatly complicates the analysis.

An important issue is the heating of the polar cap due to bombardment of the stellar surface by the downward-moving particles (Harding & Muslimov 2001). Heating of the polar cap is an important point, particularly because of the implications for X-ray observations, but we cannot discuss it quantitatively because we do not treat the escape of particles from the gap region explicitly in the model. Nevertheless, superficially it seems that there should be a large return flux to the surface and that this is a potentially serious problem for the model. We suggest two arguments against this. First, each individual electron and positron oscillates about a mean position, which is assumed to be confined to the gap region. A backward-moving particle propagates a relatively short distance before being turned around by the electric field, so that most backward-propagating particles never reach the stellar surface. This is clearly seen in the example presented in Figure 6, where the electric field vanishes at the boundaries of the gap at all times. In this case we find that the number density of the oscillating particles at the gap boundaries does not change with time (it is determined by the direct current j_0 flowing through the oscillating plasma blob) and is much smaller than in the central region, where the amplitude of the electric field is large. Below the lower boundary there are essentially no backward-moving pairs. Second, we picture the oscillations as being transient on any given field line and spatially limited in the transverse direction. Then, heating of the polar cap due to any return flux at any given time affects only a small fraction of the area of the polar cap.

The neglect of escape of particles from the gap region is due to the assumption that the oscillations are purely temporal. Hence, unfortunately, we are unable to study propagation effects leading to escape of particles, either to infinity or to the stellar surface. In a more general treatment the oscillations would be propagating as waves. A purely temporal oscillation corresponds to an infinite phase speed and zero group speed, precluding escape. Allowing the oscillations to vary in space and time (see eq. [5]), so that both a frequency ω and wave-number k can be ascribed to them, is not likely to lead to major

changes in the nature of the oscillations. Provided that the phase speed satisfies $\omega/k > c$, there exists an inertial frame in which the oscillations are purely temporal (Rowe 1995), and in that frame the oscillations should be well described by the results of the present paper. The additional effect that needs to be included involves an outward drift of this frame, at kc^2/ω , allowing escape of the particles.

The possible observational implications of the model are not as straightforward as they might at first appear. Superficially, one might expect the large-amplitude oscillations to be reflected in temporal structures in the observed emission. For example, one could argue that the period of the oscillations is plausibly of the same order as the timescale of the variations observed in the microstructure in the radio bursts. However, the emission pattern is strongly dependent on relativistic beaming effects, and the underlying oscillation frequency cannot be readily deconvolved from the Doppler effect and relativistic beaming. A specific prediction of the model arises from the approximate symmetry between upward- and downward-propagating particles: this suggests that one might observe emission from downward-propagating particles above the pole on the opposite side of the compact object to the observer. However, in order to see high-energy emission from the opposite hemisphere, the ray path must not intersect the compact object. To see radio emission, not only must the ray miss the star, but it must also pass through

the region of closed field lines around the star, where it can be absorbed or scattered through a variety of processes. As discussed above, the flux of diffusing particles impinging on the star might heat the polar cap region, and this can lead to observable thermal X-ray emission. A careful analysis of the predictions of the model are needed before one can test it and compare it with more conventional gap-plus-PFF models, for which predictions are also uncertain.

The oscillatory model raises some interesting possibilities in connection with the radio emission mechanism. Two mechanisms favored by the model are linear acceleration emission (Melrose 1978; Rowe 1995) associated with the large-amplitude oscillations and plasma-type emission at the phase where the relative flow of the electrons and positrons is nonrelativistic and Langmuir waves can grow and be converted into escaping radiation (Weatherall 1994). These and other possible radio emission mechanisms require a more detailed discussion than is appropriate here.

A. L. thanks J. Arons, V. Beskin, and V. Usov for enlightening discussions and the referee for useful comments. This research was supported in part by an ISF grant for the Israeli Center for High Energy Astrophysics and by Australian Research Council grant DP0210352.

REFERENCES

- Arendt, P. N., Jr., & Eilek, J. A. 2002, *ApJ*, 581, 451
 Arons, J. 1981, *ApJ*, 248, 1099
 Arons, J., & Scharlemann, E. 1979, *ApJ*, 231, 854
 Beskin, V. S. 1982, *Soviet Astron.*, 26, 443
 ———. 1999, *Phys.-Uspekhi*, 42, 1071
 Beskin, V. S., Gurevich, A. V., & Istomin, Ya. N. 1993, *Physics of the Pulsar Magnetosphere* (Cambridge: Cambridge Univ. Press)
 Blaskiewicz, M., Cordes, J. M., & Wasserman, I. 1991, *ApJ*, 370, 643
 Cheng, K. S., Ho, C., & Ruderman, M. A. 1986, *ApJ*, 300, 522
 Fawley, W. M., Arons, J., & Scharlemann, E. T. 1977, *ApJ*, 217, 227
 Gangadhara, R. T., & Gupta, Y. 2001, *ApJ*, 555, 31
 Harding, A. K., & Muslimov, A. G. 1998, *ApJ*, 508, 328
 ———. 2001, *ApJ*, 556, 987
 Hibschan, J. A., & Arons, J. 2001, *ApJ*, 560, 871
 Krause-Polstorff, J., & Michel, F. C. 1985, *A&A*, 144, 72
 Luo, Q. 1996, *ApJ*, 468, 338
 Melrose, D. B. 1978, *ApJ*, 225, 557
 Mestel, L. 1999, *Stellar Magnetism* (Oxford: Clarendon)
 Michel, F. C. 1991, *Theory of Neutron Star Magnetospheres* (Chicago: Univ. Chicago Press)
 ———. 2004, *Adv. Space Res.*, 33, 542
 Muslimov, A. G., & Harding, A. K. 1997, *ApJ*, 485, 735
 Romani, R. 1996, *ApJ*, 470, 469
 Rowe, E. T. 1995, *A&A*, 296, 275
 Ruderman, M. A., & Sutherland, P. G. 1975, *ApJ*, 196, 51
 Shibata, S. 1991, *ApJ*, 378, 239
 Shibata, S., Miyazaki, J., & Takahara, F. 1998, *MNRAS*, 295, L53
 ———. 2002, *MNRAS*, 336, 233
 Sturmer, S. J. 1995, *ApJ*, 446, 292
 Sturrock, P. A. 1971, *ApJ*, 164, 529
 Weatherall, J. C. 1994, *ApJ*, 428, 261
 Zhang, B., & Harding, A. K. 2000, *ApJ*, 532, 1150